

Heating effects of low power Surface Plasmon Resonance sensors

F. Galvez¹, D. Pérez de Lara², J. Spottorno^{1,4}, M. A. García^{3,4} and J. L. Vicent^{1,2}

¹Dpto. de Física de Materiales, Universidad Complutense de Madrid, 28040 Madrid, Spain

²IMDEA-Nanociencia, Campus Cantoblanco, 28049 Madrid, Spain

³Instituto de Cerámica y Vidrio, Consejo Superior de Investigaciones Científicas, 28049 Madrid, Spain

⁴ Instituto de Magnetismo Aplicado 'Salvador Velayos', Universidad Complutense de Madrid, 28230 Madrid, Spain

Abstract

We present here a study of the possible local heating effects in surface plasmon resonance sensors using low power lasers ($\sim \text{mW/mm}^2$). By measuring the increase of electrical resistivity in an Au stripe while exciting SPR and performing numerical simulations we determine upper limits to the local heating that result of the order of $\sim 0.1 \text{ K}$ and $\sim 1 \text{ K}$ for laser power densities of 1.5 mW/mm^2 and 15 mW/mm^2 respectively.

Keywords: Surface plasmons, local heating, sensors

1. Introduction

Surface plasmon resonance (SPR) consists in a collective oscillation of conduction electrons at metal dielectric-interface [1,2,3,4]. For the case of noble metals, this resonance is very weakly damped and consequently, very sensitive to any modification of the external environment. Therefore, SPR is the base of many sensors [5,6,7]. The most widely used configuration is the SPR on metallic films, where the adsorption of chemical species on top of a functionalized Au film yields measurable changes in the resonance conditions [5,8].

The excitation of SPR in metallic films leads to a concentration and local amplification of electromagnetic energy in very small regions above the diffraction limit [9,10]. For the case of noble metal films, when SPR is excited, the electromagnetic field at the metal/dielectric interface can be up to 80 times that of the incident light [2]. This energy stored in form of surface plasmons can be released via re-emission of light or heat dissipation. When the heat dissipation is the main mechanism for energy release, this can lead to intense local heating, due to the locally very high energy density [2,11,12].

Therefore, when SPR is used for sensing, local heating may alter processes leading to erroneous results since the gas and molecular absorption/desorption rates on a functionalized surface depend on the local temperature [13,14].

Consequently, in SPR based sensors, low-power density light sources ($\sim \text{mW}/\text{mm}^2$) are commonly used to minimize possible thermal effects. Nevertheless, it is important to determine the local increase of temperature upon SPR excitation when using low-power light sources in order to determine to what extent it can affect to the resolution and sensitivity of the measurements.

In this paper we study the local heating induced in Au films upon excitation of SPR with low power lasers as those used for sensors (typically $\sim 1\text{-}15\text{mW}/\text{mm}^2$). To this purpose we measure the electrical resistivity of the film upon SPR excitation and determine the local increase of temperature. This electrical measurement seems the most appropriated one as it is highly non-invasive. Since we are studying the heating in a small Au element with $\sim 40\text{ nm}$ thickness,

the mass of the thermocouple or other probe would be huge in comparison with the mass of the Au film so it would modify the temperature distribution. In addition, excitation of SPR requires from a very particular optic configuration and any element in direct contact with the Au film surface alters and damps the excitation of SPR. That is the reason why we choose measurement of resistivity as the suitable probe to measure the local heating that has no effect on the optical configuration of the system. We also present here simulations of the local heating process that are compared with the experimental results.

2. Experimental

Sample consisted in a nominal 40 nm Au film deposited on sodalime glass substrate by e-beam evaporation using a mask and subsequently patterned in the shape of a strip 2 mm wide. The patterning was carried on using UV photolithography to define a protective resist layer with the desired shape, followed by a wet etching process in *aqua regia* solution for a few seconds then rinsed in deionized water and acetone in order to stop the etching and clean the remaining resist layer. Finally, silver colloid was used to attach four electrical contacts aligned along the strip so that a bigger gap is left between the 2nd and 3rd contact for the laser spot to be focused right there, as shown in Fig. 1b.

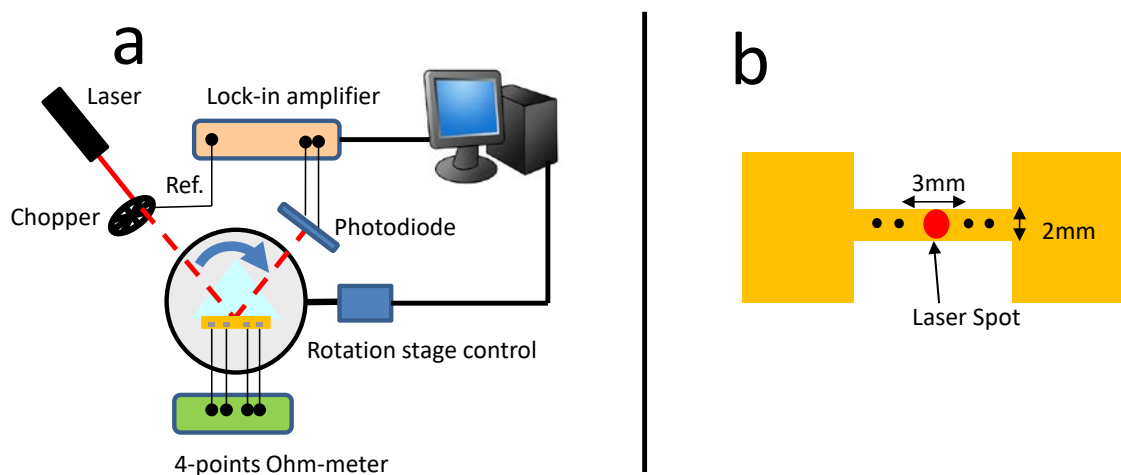


Figure1 (a) Scheme of the SPR device with 4-points resistance measurement system. (b) Illustration of the sample geometry with the four contacts.

SPR were measured with a home-made device described elsewhere [15]. Two different lasers were used. A solid diode laser with 543 nm wavelength and HeNe laser operating at 632.8 nm. The power of the polarized laser beams were 15 mW and 1.5 mW respectively and the spot exhibits a Gaussian profile with 1 mm full-width-half maximum (FWHM).

This set-up was modified including the possibility to measure electrical resistance using a four points configuration. Visual Basic codes were developed to allow measurements of the electrical and SPR signals as a function of time and incidence angle. Figure 1a shows a sketch of the device.

3. Results and Discussion

Figure 2 shows the SPR spectrum of the sample measured with a red HeNe laser on the sample.

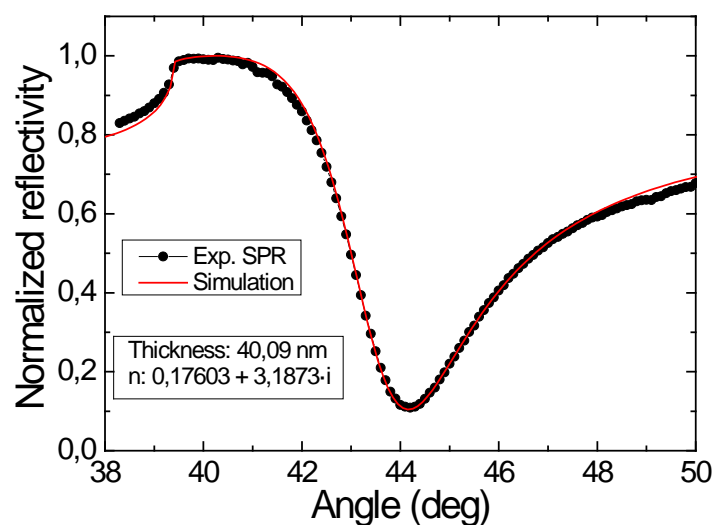


Figure 2. SPR spectrum of the sample measured with a HeNe laser (632.8 nm) and the best fit obtained with the parameters indicated in the figure.

The spectrum can be fitted assuming a thickness of 40.1 nm and refractive index very close to those reported for Au in literature [16] that is indicated in the figure.

In the first experiment, we measured the electrical resistance when illuminating the sample at resonant conditions (44.2 deg incidence angle) and modulating the illumination with pulses of 10 seconds and 10 seconds without illumination.

In this way we can separate the effects of SPR excitation from other possible experimental artifacts. Figure 3 shows the result of these measurements.

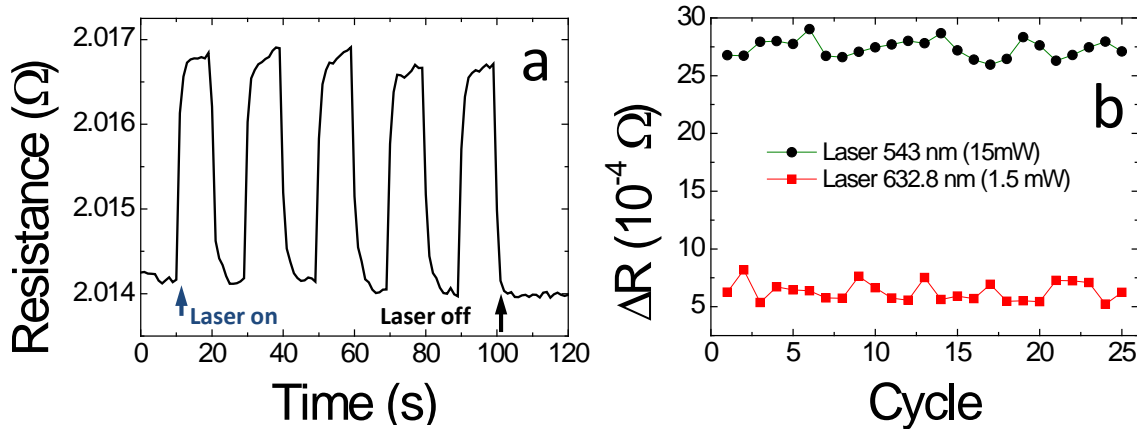


Figure 3. (a) Resistivity of the sample illuminating with a 543 nm laser ($15 \text{ mW}/\text{mm}^2$) in SPR conditions and modulating the light with 10 seconds intervals (b) Resistance variations produced by laser illumination in SPR conditions for two different lasers.

The electrical resistance of the sample increases when it is illuminated in conditions of SPR excitation. The increase of temperature follows the modulation of the light and disappears when the illumination is removed. This behavior demonstrates that the jumps observed on the resistance in figure 3a are associated with the illumination. In figure 3b we present the value of the jumps observed in the electrical resistance of the sample. Those changes are about $6.3 \cdot 10^{-4} \Omega$ and $2.7 \cdot 10^{-3} \Omega$ for the red (1.5 mW) and green (15 mW) lasers respectively.

We performed additional control experiments to check that the measured resistance variation are associated with the excitation SPR and no other process related to illumination, for instance optical absorption to promote interband transition in the gold stripe [17] or absorption due to silica defects [18,19,20].

The first one consisted on recording the electrical resistance when varying the incidence angle of the laser as we do when measuring the SPR spectrum in figure 1. In this experiment the light was also modulated with 10 seconds pulses

in order to separate the effects of SPR excitation from other possible effects. The results of this experiment are presented in Figure 4.

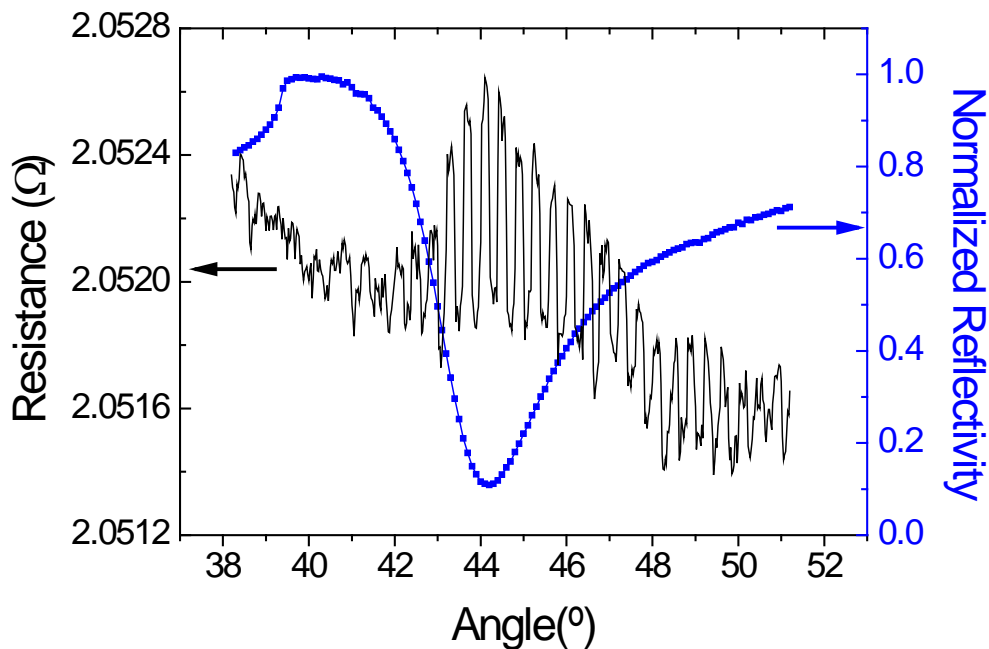


Figure 4.Electrical resistance of the sample when illuminating with the laser as a function of the incidence angle with modulated light. The SPR spectrum is also presented for comparison purposes.

The electrical resistance of the sample exhibits time variations that match the modulation of the light. Those variations are maxima at resonant conditions and reduce up to disappear when we are totally out of the resonance. Additionally, we repeated the measurement illuminating the sample with the laser with p-polarization that is not able to excite SPR. In this case, no changes in the resistance were observed upon light illumination irrespective of the incidence angle. Consequently, we can associate the resistance variations measured here to the excitation of SPR disregarding any other optical process.

In order to calculate the local temperature that the Au film reaches upon SPR excitation we considered initially two extreme situations to get lower and upper limits.

The first situation that provides a lower limit is to assume that the whole region for which the electrical resistance is measured is heated homogeneously. The tabulated electrical resistivity for Au is $2.44 \cdot 10^{-8} \Omega \cdot m$ and around room temperature the thermal dependence of the resistivity is of $8.1 \cdot 10^{-11} \Omega \cdot m \cdot K^{-1}$

[21]. For a gold element with 2x3 mm area and 40 nm thickness the resistance is 0.915 Ω and its thermal dependence should be $6.03 \cdot 10^{-3} \Omega \cdot K^{-1}$. Therefore, the increase of the resistance of $6.3 \cdot 10^{-4} \Omega$ observed upon SPR excitation with the red laser of 1.5 mW should correspond to an increase of temperature of the spot region of $\Delta T = 0.104$ K. Similarly for the green laser with power of 15 mW, the measured increase of resistance of $2.7 \cdot 10^{-3} \Omega$ would correspond to an increase of $\Delta T = 0.43$ K.

The second situation that provides an upper limit corresponds to assume that just the region directly illuminated by the laser results heated. As the spot has a Gaussian profile with a 1 mm FWHM, we assume that a region with 1 mm radius (that receives 95.5% of the power) is heated while the rest of the material remains unchanged. The calculation of the thermal dependence of the resistance results complicated for this geometry and is detailed in Appendix 1. According to the calculations, when exciting SRP with the 1.5 mW laser, the local increase of temperature at the spot region results $\Delta T = 0.39$ K while for the 15 mW green laser the overheating is $\Delta T = 1.69$ K.

Finally, we performed a simulation using COMSOL software. For this calculation we considered an Au stripe with the dimensions of our system (2 mm width, 40 nm thickness) over a soda-lime glass (1 mm thick) and a heat focus with power 1.5 mW and 15 mW that is dissipated on a disk with 1 mm radius and 40 nm thickness (see figure 5a). We assumed room temperature to be 300 K and a heat transfer coefficient Au/air of $30 \text{ W} \cdot \text{K}^{-1} \cdot \text{m}^{-2}$. Figure 5 shows the temperature distribution at the stationary state. For the 1.5 mW power the maximum increase of temperature takes place at the center of the spot and results to be $\Delta T = 0.12$ K, while in the case of the 15 mW laser this increase is $\Delta T = 1.22$ K.

The temperature distributions along a line parallel to the stripe (dashed line in the figure 5a) are shown in figure 5c&5d. We found that the temperature decreases from the center of the spot as expected. For the 1.5 mW laser the temperature at a distance of 5 mm from the center of the spot increases about $\Delta T = 0.06$ K while for the 15 mW laser it is $\Delta T = 0.6$ K.

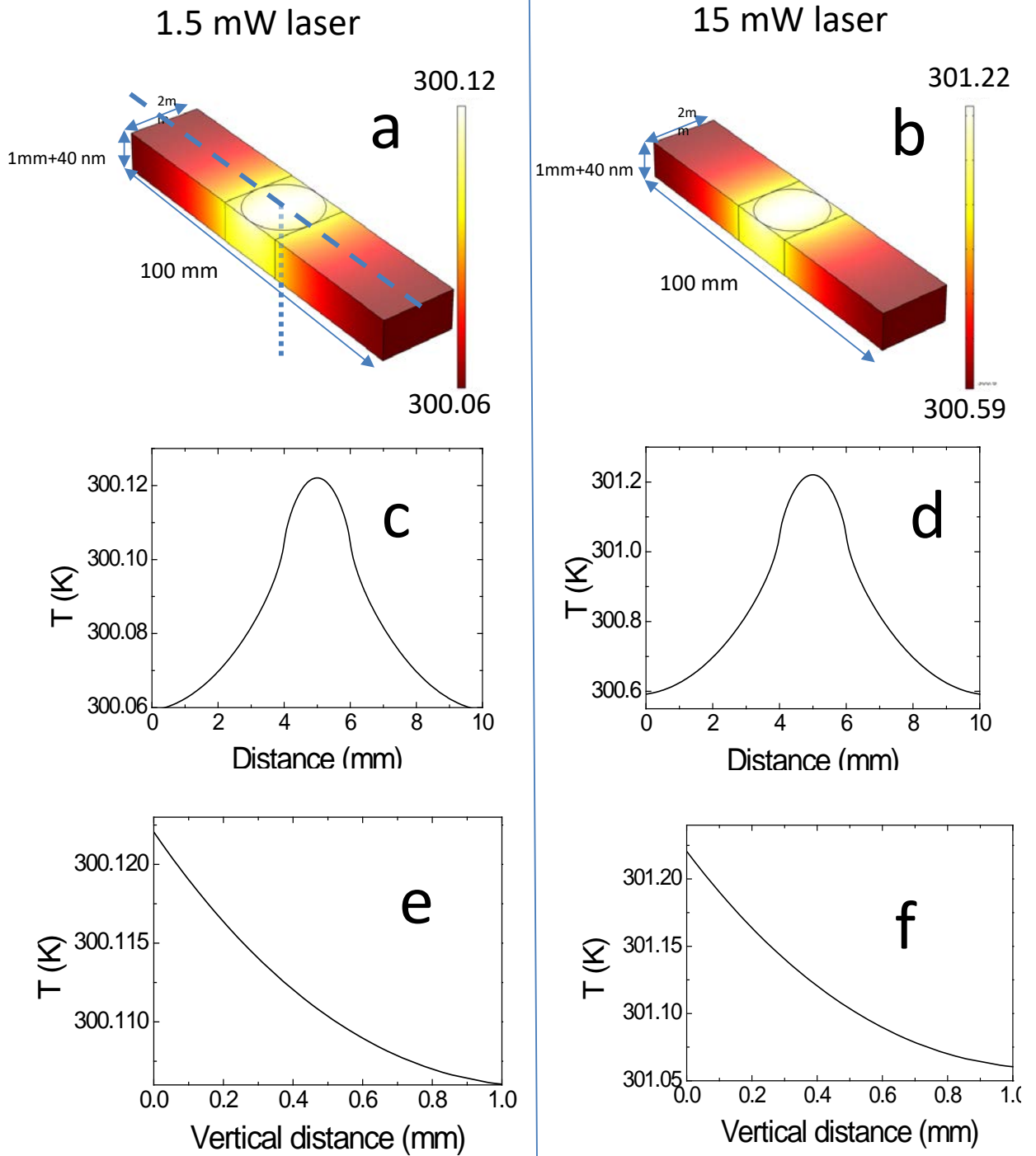


Figure 5. Simulation of the distribution of temperatures upon SPR excitation with (left) 1.5 mw laser and (right) 15 mw laser. (a,b) False color temperature images; (c,d), temperature distribution along a central straight line parallel to the stripe direction (dashed line in panel a); (e,f) temperature distribution along a vertical line at the center of the spot (dotted line in panel a).

These temperatures obtained from the simulation exhibit a reasonable agreement with the experimental data, falling in between the upper and lower limits above calculated from the electrical measurement.

The key difference between experimental and calculation theories is that according to the simulation the increase of temperature is lineal with the laser power while from the experimental data we found that by increasing a factor of 10 the laser power (from 1.5 mW to 15 mW), the temperature increases about a factor 4. This difference may be due to the fact that upon excitation of SPR, a part of the energy absorbed by the system is re-emitted as light [2], while in our calculation we assumed all the laser power to be dissipated inform of heat. This re-emission is not a linear effect and increases with the incident light intensity. Thus, an increase of a factor 10 in the laser power do not yield the same increase in the dissipated power, explaining the lower heating observed in the experimental measurements.

While experimental data on electrical conductivity only provide information about heating of the conductive Au film, the simulation also allows estimating the heating of the glass substrate. From figures 5e & 5f we found that the substrate results significantly heated up to a depth of 1 mm. The average increase of temperature results of $\Delta T = 0.11$ K and $\Delta T = 1.1$ K for the 1.5 mw and 15 mW laser respectively. Considering that about room temperature, the refractive index of silica based glasses the refractive index is about 1.52 and has a thermal dependence of $\sim 10^{-5} \text{ K}^{-1}$ [22], the modification of the refractive index results of the order $10^{-5} - 10^{-6}$. Such a modification can be considered as negligible as concerns the excitation of SPR.

4. Conclusions

We estimated the local increase of temperature when exciting SPR on Au films with low-power sources. From experimental data and simulations, we found that local increase of temperature at the laser spot position are below ~ 0.1 K and ~ 1 K for laser power flux of the order of 1.5 mW/mm^2 and 15 mW/mm^2 respectively, for sensors working in air. Lower values are expected for sensors

in liquid media. Thus, when using SPR for sensing purposes, those values may be used to provide limits to the possible thermal effects that could modify the response of the system.

5. Acknowledgments

This work has been supported by the Ministerio Español de Economía y Competitividad (MINECO) MAT2013-48009-C4-1 and FIS2013-45469-C4-1 and Comunidad de Madrid (CM) S2013/MIT-2850. MAG also acknowledges financial support from BBVA foundation.

Appendix A

Calculation of the resistivity of a thin film with a circular region heated.

Consider the situation described by the figure 6 with a film with length L , width W and thickness T , in which a circular region of radius $R=W/2$ is heated homogeneously.

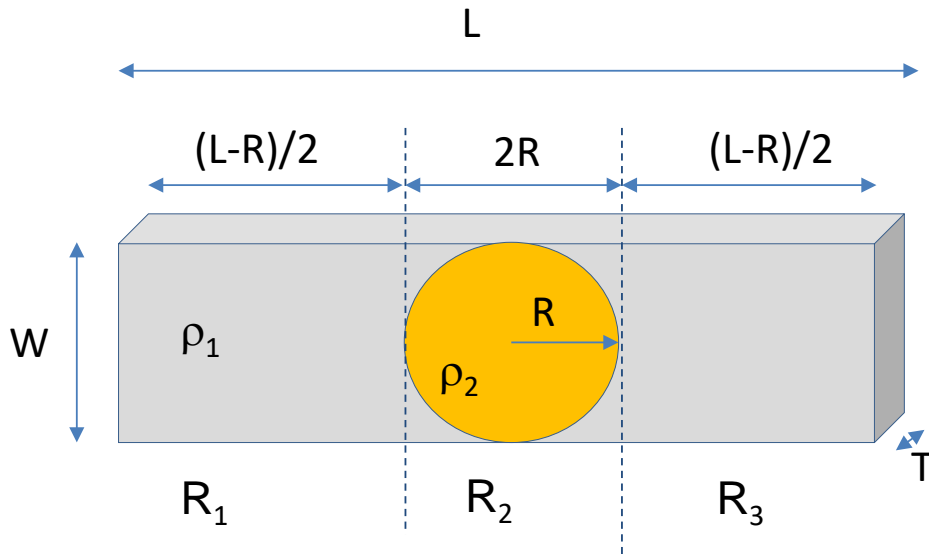


Figure 6 Scheme of the analyzed element

The electrical resistance of the element can be obtained assuming an inhomogeneous material with resistivity ρ_1 out of the circle and ρ_2 inside the circle. The total of the element will be the sum of 3 resistances in series corresponding to regions 1, 2 and 3. For the regions 1 and 3 it is straightforward that resistance will be:

$$R_1 = R_3 = \rho_1 \cdot \frac{(L-R)}{2 \cdot W \cdot T} (1)$$

As concerns R_2 it can be obtained as the sum of the resistance of thin films sections with length dx as described in the figure 7. Actually each section corresponds to the sum of three resistances in parallel, two of them identical corresponding to the region with resistivity ρ_1 and one with resistivity ρ_2 .

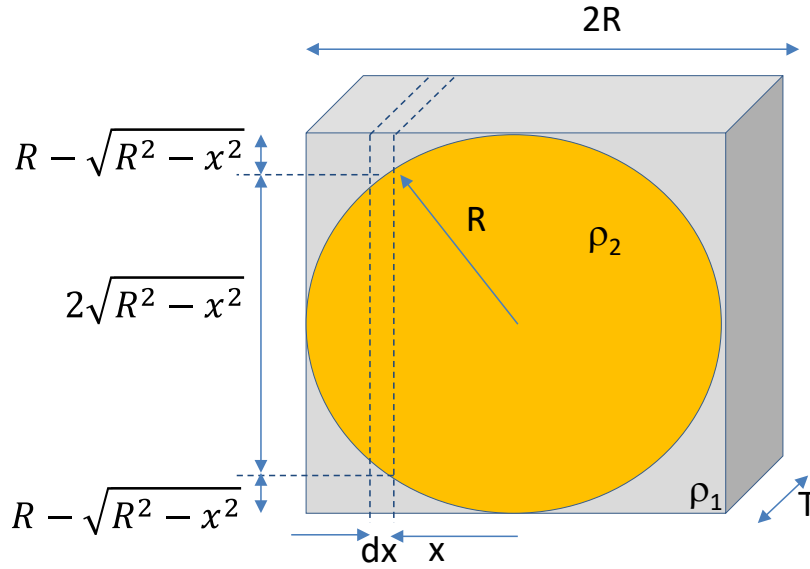


Figure 7 Scheme and dimension of the finite elements considered to calculate the total resistance of the section 2.

$$R_2 = \int_{-R}^R \left(\frac{2}{\rho_1 \cdot \frac{dx}{T \cdot (R - \sqrt{R^2 - x^2})}} + \frac{1}{\rho_2 \cdot \frac{dx}{T \cdot 2R \cdot \sqrt{R^2 - x^2}}} \right)^{-1} =$$

$$\int_{-R}^R dx \left(\frac{2T \cdot (R - \sqrt{R^2 - x^2})}{\rho_1} + \frac{2T \cdot \sqrt{R^2 - x^2}}{\rho_2} \right)^{-1} \quad (2)$$

If we set ρ_1 as the tabulated resistivity for Au at 300 K, $T=40$ nm, and $R=1$ mm, and solve numerically this integral we obtain the linear relationship between R_2 and ρ_2 shown in figure 8:

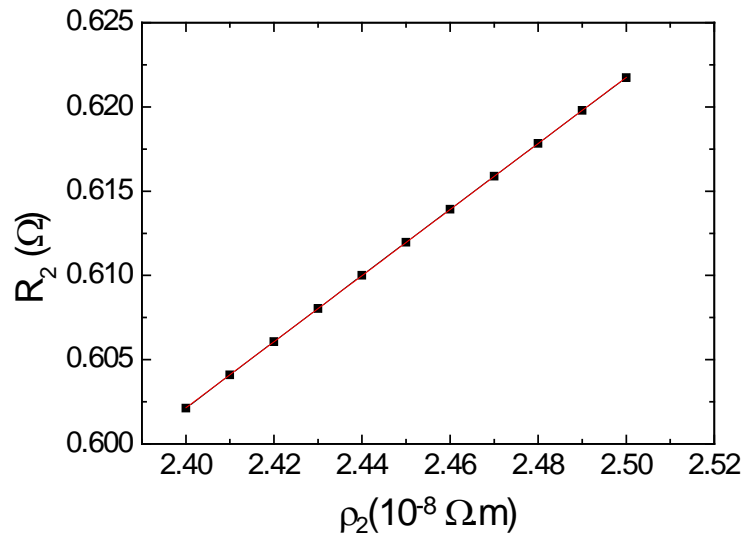


Figure 8 Resistance R_2 as a function of the resistivity in the disk ρ_2 according to Eq. (2).

From a linear fit we obtain the following relationship:

$$\rho_2 = (5.099 \cdot R_2 - 0.67) \cdot 10^{-8}$$

Since R_2 is the only term of the total resistance that varies its value (assuming just heating of the laser spot area) the increase of resistance experimentally measured corresponds to this term. Therefore, the observed increase of resistance upon illumination with the 1.5 mW laser of $\Delta R_2 = 6.3 \cdot 10^{-4} \Omega$ correspond to an increase of resistivity of $\Delta \rho_2 = 3.2 \cdot 10^{-11} \Omega \cdot \text{m}$. Since the thermal dependence of the resistivity for Au is $8.1 \cdot 10^{-11} \Omega \cdot \text{m} \cdot \text{K}^{-1}$, this corresponds to an increase of the temperature of the disk of $\Delta T = 0.39 \text{ K}$. Similarly, for the case of the green 15 mW laser the increase of resistance of $\Delta R_2 = 2.7 \cdot 10^{-3} \Omega$ yields $\Delta \rho_2 = 1.3 \cdot 10^{-10} \Omega \cdot \text{m}$ and $\Delta T = 1.69 \text{ K}$.

References

- 1 U. Kreibig, M. Vollmer, *Optical Properties of Metal Clusters*(Springer-Verlag, Berlin, 1995)
- 2H. Raether, *Surface Plasmons on Smooth and Rouge Surfaces and on Gratings* (Springer-Verlag, Berlin, 1988)
- 3 W. Knoll, *Annu Rev Phys Chem.*, **49** (1998) 569.
- 4 M. L. Brongersma and P. G. Kik, *Surface Plasmon Nanophotonics* (Springer-Verlag, Berlin, 1988).
- 5J. Homola, S. S. Yee, G. Gauglitz, *Sensors and Act. B Chem.* **54** (1999) 3.
- 6B. Liedberg, C. Nylander, I. Lunström *Sensors and Act.***4** (1983) 299.
- 7 K. A. Willets, R. P. Van Duyne *Ann. Rev. of Phys. Chem.* **58** (2007) 267.
- 8 C. Nylander, B. Liedberg, T. Lind *Sensors and Act.* **3** (1982-1983) 79.
- 9 W. L. Barnes, A. Dereux, T. W. Ebbesen *Nature* **424** (2003) 824.
- 10 J. A. Schuller, E. S. Barnard,W. Cai, Y. Chul Jun, J. S. White, M. L. Brongersma *Nat. Mat.* **9** (2010)193.
- 11L. Röntzsch, Karl-Heinz Heinig, J. A. Schuller, M. L. Brongersma, *Appl. Phys. Lett.* **90** (2007) , 044105.
- 12 D. K. Roper , W. Ahn , M. Hoepfner *J. Phys. Chem. C*, **111**(2007) 3636.
- 13 L. K. Lee, D. M. Ruthven, *J. Chem. Soc., Faraday Trans. 1*, **75** (1979) 2406.
- 14 E. Reimhult , F. Höök , B. Kasemo *Langmuir*,**19** (2003), 1681.
- 15 A. Serrano, O. R. de la Fuente, and M. A. Garcia, *J. Appl. Phys.* **108** (2010)074303.
- 16 P. B. Johnson, R. W.Christy *Phys. Rev. B* **6** (1972) 4370.
- 17 P. G. Etchegoin, E. C. Le Ru,M. Meyer, *J. Chem Phys.* **125** (2006) 164705.
- 18 L. Skuja *Optical Properties of Defects in silica*, in *Defects in SiO₂ and Related Dielectrics: Science and Technology*, NATO Science Series Volume 2 2000; Spinger (2000)
- 19 H. Nishikawa, R. Tohmon, Y. Ohki, K. Nagasawa, Y. Hama, *J. Appl. Phys.***65** (1989) 4672.
- 20 C. D. Marshall, J. A. Speth, S. A. Payne, *J. Non-Cryst. Solids* **212** (1997) 59.
- 21 D. R. Lide, . *Handbook of Chemistry and Physics*. 75th Edition. New York: CRC Press, 1996-1997: 11-41.
- 22 Douglas B. Leviton and Bradley J. Frey ; *Proc. SPIE 6273, Optomech. Techn. Astr.* 62732K (2006).